Edge magnetoplasmons for very low temperatures and sharp density profiles

O. G. Balev

Institute of Physics of Semiconductors, National Academy of Sciences, 45 Prospekt Nauky, Kiev 252650, Ukraine

P. Vasilopoulos

Department of Physics, Concordia University, 1455 de Maisonneuve Boulevard O, Montréal, Québec, Canada, H3G 1M8

A treatment of edge magnetoplasmons (EMP), based on a *microscopic* evaluation of the local contributions to the current density, is presented. It is valid in the quantum Hall regime for filling factor $\nu=1$ or 2 and low temperatures when the dissipation is localized near the edge. The confining potential, flat in the interior of the channel, is assumed smooth on the magnetic length ℓ_0 scale, but sufficiently steep at the edges that the density profile is sharp and the dissipation considered results only from electron *intraedge-intralevel* transitions due to scattering by piezoelectrical phonons. For wide channels there exist independent EMP modes spatially *symmetric* or *antisymmetric* with respect to the edge. Certain of these modes can propagate nearly undamped, even when the dissipation is strong, and are thus termed *edge helicons*. In contrast with well-known results for a spatially homogeneous dissipation within the channel, we obtain that the damping of the fundamental EMP is not quantized and varies as T^3 or T^{-3}, where T is the temperature, in the high- and low-frequency limits, respectively. The characteristic length of the resulting dispersion relation and of the charge density distortion is ℓ_0. The screening of the metallic gates, when present, is taken into account. [S0163-1829(97)01744-X]

I. INTRODUCTION

In the past few years there has been considerable interest in edge magnetoplasmons (EMP's) as well as in other edge excitations of two-dimensional (2D) electron systems in the presence of a magnetic field B.[1-12] For a 2D system with a vertical conductivity drop at the boundaries, it has been shown[1] that the dissipation can determine the EMP dispersion relation and the spatial structure in an essential manner even in the regime of the quantum Hall effect (QHE). In this work the properties of the EMP are expressed in terms of the components of the magnetoconductivity tensor of an infinite 2D system. Moreover, due the very low frequency ω of the EMP, the dispersion relation could be written in terms of the static magnetoconductivity tensor.

The distance of the ''center of gravity'' of the EMP charge from the edge, which coincides with the characteristic length over which the transverse to the edge electric field E_y of the EMP decreases, is given, for $|k_x\ell_v|\ll1$, by[1]

$$\ell_{vc}=\frac{|\ell_v|}{\pi}\left[\ln\left(\frac{2}{|k_x\ell_v|}\right)+1\right]=\left|\frac{\sigma_{yy}}{k_x\sigma_{yx}}\right|. \tag{1}$$

Here σ_{yy} and σ_{yx} are the conductivity components of an infinite 2D system, k_x is the EMP wave vector, and ℓ_v denotes a characteristic length determined by Eq. (10) of Ref. 1. In the QHE regime for typically observed[7] EMP, Eq. (1) gives $\ell_{vc}\lesssim1$ μm. In Ref. 13 we showed theoretically, and in agreement with experimental observations, that in the QHE regime and for sufficiently smooth confinement the dissipation is due to intralevel-intraedge transitions of electrons scattered by piezoelectrical phonons and occurs mainly near the edges of channels. In the linear-response regime this is the main dissipation for channels of width $W\lesssim100$ μm and temperatures $T\lesssim1$ K if the group velocity of edge states, v_g,

is larger than the speed of sound s. As for dissipation in the bulk, it is exponentially suppressed for $T\rightarrow0$. Given that and the fact that the dissipation, when deriving Eq. (1), occurs in the bulk, we expect the properties of the EMP to be strongly modified when the dissipation is localized near the edges.

The above expectation is further supported by the results of Ref. 11, which pertain to EMP's for a smooth, unperturbed electron density profile which contrasts sharply with that of Ref. 1 where the density drops vertically at the edges. In addition to the modes of Ref. 1, acoustic EMP's were obtained in Ref. 11. Further, our results, despite their partial similarity with those of Refs. 1 and 11, show significant differences from them even when the dissipation is very weak. For the very low temperatures that we consider here, $k_BT\ll\hbar v_g/\ell_0$, and the assumed smooth confining potential on the scale of ℓ_0 ($v_g>s$), the unperturbed electron density $n_0(y)$, normalized to the bulk value n_0, drops essentially, on the scale of ℓ_0, only near the edge. More explicitly, for the potential that is specified at the beginning of Sec. II, we calculate $n_0(y)/n_0=\{1+\Phi[(y_{re}-y)/\ell_0]\}/2$, where y_{re} is the coordinate of the right edge, and $\Phi(y)$ the probability integral. In Fig. 1 we show this calculated density profile (short-dashed curve) together with those assumed in Refs. 1 (solid curve) and 11 (long-dashed curve). The profile of Ref. 11 is obtained with $n_0(y)/n_0=(2/\pi)\arctan\sqrt{(y_{re}-y)/a}$ and $a/\ell_0=20$; it corresponds approximately to $a=2000$ Å. As can be seen, the three density profiles are very different from each other. As will be shown in this paper, combining our density profile with the localization of the dissipation near the edge leads to strong modifications of the EMP results.

These modifications, as well as new EMP's resulting from the microscopic treatment of the problem, are the subject of this work. The description of the inhomogeneous current density in the quasistatic regime is carried out using the results of Ref. 14. We consider the QHE regime, mainly ν
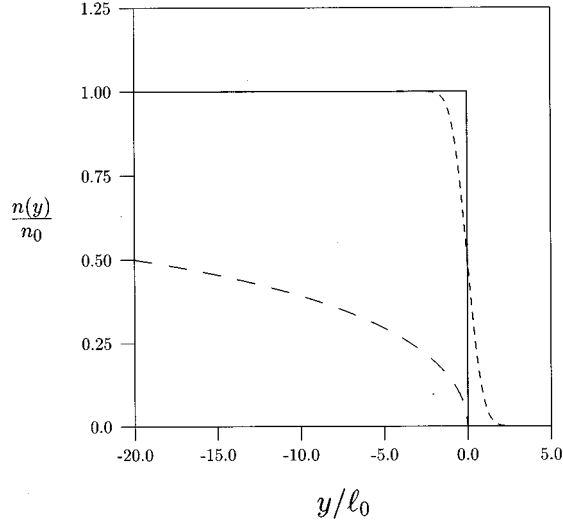

FIG. 1. Unperturbed electron density $n_0(y)$, normalized to the bulk value n_0, as a function of $\overline{y}/\ell_0$ measured from the right edge taken as the origin. The solid and long-dashed curves are obtained from the models of Refs. 1 and 11, respectively, as explained in the text. The short-dashed curve is the profile of the present work.

$=1$ and partly $\nu=2$, for samples with sufficiently large in-plane dimensions, as is typical in EMP experiments, that interedge electron transitions and the interedge Coulomb interaction can be neglected.

In Sec. II we start with expressions for the inhomogeneous current densities and conductivities, and derive the integral equation for EMP's. In Sec. III we derive the dispersion relation for very low temperatures, and in Sec. IV we describe in detail the new edge waves. Finally, in Sec. V we compare our theory with the experiment and make concluding remarks.

II. BASIC RELATIONS

A. Inhomogeneous current density in quasistatic regime

We consider a two-dimensional electron gas (2DEG), of width W, of length $L_x=L$, and of thickness zero, in the presence of a strong magnetic field B parallel to the z axis. The 2DEG is confined along the y axis. For simplicity we take the confining potential as parabolic at the edges: $V'_y=0$, for $y_l<y<y_r$, $V'_y=m^*\Omega^2(y-y_r)^2/2$ for $y>y_r>0$, and $V'_y=m^*\Omega^2(y-y_l)^2/2$ for $y<y_l<0$. Because in real EMP experiments $W\gtrsim0.1$ cm, we can assume $[W-(y_r-y_l)]/W\ll1$. Moreover, we will assume that $|k_x|W\gg1$, such that it is possible to consider an EMP along the right edge of the channel, of the form $A(\omega,k_x,y)\exp[-i(\omega t-k_xx)]$, totally independent of the left edge. We consider only linear responses. For definiteness, we take the background dielectric constant ϵ to be spatially homogeneous. We consider B strong enough that only the $n=0$ Landau level (LL) is occupied. For the $\nu=2$ QHE regime we will neglect the spin splitting. As for the $\nu=1$ QHE, we will assume that the spin splitting, caused by many-body effects, is strong enough to neglect the contribution related with the upper spin-split LL. We assume a lateral confinement smooth on the scale of the magnetic length $\ell_0=(\hbar/m^*\omega_c)^{1/2}$ such that $\Omega\ll\omega_c$, where

$\omega_c=|e|B/m^*$ is the cyclotron frequency. Further, we will approximate $\widetilde{\omega}=(\omega_c^2+\Omega^2)^{1/2}$ by ω_c.

Because the EMP is practically quasistatic and its wavelength $\lambda\gtrsim1$ cm is very large, we expect, in analogy with well-known results that follow from Maxwell's equations,[15] the associated electric field $E_x(x,y,t)$ to have a smooth dependence on y on the scale of $\ell_0=(\hbar/m^*\omega_c)^{1/2}$, i.e., $E_x(x,y,t)=E_x(y)\exp[-i(\omega t-k_xx)]$. Physically is clear: the dependence of $E_x(x,y,t)$ on y, as expressed through Maxwell's equations, is related to that on x which has a characteristic scale λ. Thus $E_x(y)$ should have the same scale λ and be definitely smooth on the ℓ_0 scale. This is a general result and applies to the case treated in Ref. 1. Then using the results of Ref. 14, we obtain the components of the current density in the forms

$$j_y(y)=\sigma_{yy}(y)E_y(y)+\sigma_{yx}^0(y)E_x(y), \qquad (2)$$

$$j_x(y)=\sigma_{xx}(y)E_x(y)-\sigma_{yx}^0(y)E_y(y)+v_g\rho(\omega,k_x,y). \qquad (3)$$

Here we suppressed the exponential factor $\exp[-i(\omega t-k_xx)]$ common to all terms in Eqs. (2) and (3). It is understood that $E_\mu(y)$ depends on ω and k_x. As follows from Refs. 13 and 14, $\sigma_{yy}(y)$ is strongly (exponentially) localized at the edge, within a distance $\lesssim\ell_0$ from it, for $\hbar v_g\gg k_BT\ell_0$. The last term on the right-hand side of Eq. (3), absent in Ref. 14, represents a convection contribution to the current density along x, associated with the wave, and is due to a distortion $\delta\rho$ of the charge localized near the edge; we denote it by $\rho(\omega,k_x,y)$ in order to simplify the notation as it occurs frequently. Notice that in Ref. 14 the contributions to the components of the current density are microscopically obtained for the electric field components smooth on the scale of ℓ_0. This condition holds for the contributions $\propto E_x(y)$ in Eqs. (2) and (3), but is not well justified for those $\propto E_y(y)$. We assume that the latter can be reasonably approximated by those obtained microscopically when $E_y(y)$ is smooth on the scale of ℓ_0. The assumption is equivalent to neglecting possible nonlocal contributions to the current density $\propto\int dy'\sigma_{\mu y}(y,y')E_y(y')$. Then it follows that $\sigma_{xy}^0=-\sigma_{yx}^0$. For $\nu=1$ we have[14]

$$\sigma_{yx}^0(y)=\frac{e^2}{2\pi\hbar}\int_{-\infty}^{\infty}dy_{0\alpha}f_{\alpha0}\Psi_0^2(y-y_{0\alpha}), \qquad (4)$$

where $\alpha\equiv\{0,k_{x\alpha}\}$, $y_{0\alpha}=\ell_0^2k_{x\alpha}$, $\Psi_n(y)$ is a harmonic oscillator function, and $f_{\alpha0}\equiv f_0(k_{x\alpha})=1/(1+\exp[(E_{\alpha0}-E_{F0})/k_BT])$ is the Fermi-Dirac function. E_{F0} is the Fermi level counted from the bottom of the lowest electric subband. For $T=0$ and near the right edge we have $\sigma_{yx}^0(y)=(e^2/4\pi\hbar)\{1+\Phi[(y_{re}-y)/\ell_0]\}$, where $\Phi(x)$ is the probability integral, $y_{re}=\ell_0^2k_{re}$, and $f_0(k_{re})=\frac{1}{2}$. That is, $\sigma_{yx}^0(y)$ near the edge decreases on the scale of ℓ_0, and behaves as the density of the short-dashed curve of Fig. 1. Considering only the right edge and the flat part of the confining potential, for $y_l\lesssim y_{0\alpha}\lesssim y_r$ we have $E_{\alpha0}=\hbar\omega_c/2$ and for $y_{0\alpha}\gtrsim y_r$ we obtain

$$E_{\alpha0}\equiv E_0(k_{x\alpha})=\hbar\omega_c/2+m^*\Omega^2(y_{0\alpha}-y_r)^2/2. \qquad (5)$$

We consider only the interaction of electrons with phonons, and neglect that with impurities, since the former is the most

essential for the assumed conditions.[13] Because of the very smooth dependence of $E_x(y)$ on ℓ_0, we can assume that $\sigma_{xx}(y)$ can be approximated by $\sigma_{yy}(y)$, which follows from Eq. (16) of Ref. 14 as

$$\sigma_{yy}(y) = \frac{\pi e^2 \ell_0^4}{4\hbar L k_B T} \sum_{k_{x\alpha}\mathbf{q}} |C_\mathbf{q}|^2 q_x^2 [f_0(k_{x\alpha} - q_x) - f_0(k_{x\alpha})]$$

$$\times \delta[E_0(k_{x\alpha}) - E_0(k_{x\alpha} - q_x) - \hbar\omega_{\bar{q}}] e^{-(q_x^2 + q_y^2)\ell_0^2/2}$$

$$\times \sinh^{-2}\left(\frac{\hbar\omega_{\bar{q}}}{2k_B T}\right) \{\Psi_0^2[y - y_0(k_{x\alpha} - q_x)]$$

$$+ \Psi_0^2[y - y_0(k_{x\alpha})]\}. \tag{6}$$

For the low temperatures pertinent to the quantum Hall effect, we consider only the standard acoustical (DA) or piezo-electrical (PA) phonons for which $\omega_\mathbf{q} = sq$, where s is the speed of sound, and $q = \sqrt{q_x^2 + q_y^2 + q_z^2}$. Then $|C_\mathbf{q}|^2 = (c'/L_x L_y L_z) q^{\pm 1}$, where $+1$ is for DA and -1 for PA phonons, respectively.

B. Integral equation for EMP's with dissipation at the edges

Using Eqs. (2)–(4), and (6), we can write the continuity equation, linearized in $\delta\rho(\omega, k_x, y) \equiv \rho(\omega, k_x, y)$, as

$$-i(\omega - k_x v_g)\rho(\omega, k_x, y) + ik_x[\sigma_{xx}(y)E_x(\omega, k_x, y)$$

$$- \sigma_{yx}^0(y)E_y(\omega, k_x, y)] + \frac{\partial}{\partial y}[\sigma_{yy}(y)E_y(\omega, k_x, y)$$

$$+ \sigma_{yx}^0(y)E_x(\omega, k_x, y)] = 0. \tag{7}$$

In terms of the potential $\phi(\omega, k_x, y)$ the electric-field components are $E_x(\omega, k_x, y) = -ik_x\phi(\omega, k_x, y)$ and $E_y(\omega, k_x, y) = -(\partial/\partial y)\phi(\omega, k_x, y)$. Then Eq. (7) gives

$$-i(\omega - k_x v_g)\rho(\omega, k_x, y) + k_x^2 \sigma_{xx}(y)\phi(\omega, k_x, y)$$

$$- \frac{\partial}{\partial y}\left[\sigma_{yy}(y)\frac{\partial}{\partial y}\phi(\omega, k_x, y)\right]$$

$$- ik_x\phi(\omega, k_x, y)\frac{\partial}{\partial y}\sigma_{yx}^0(y) = 0. \tag{8}$$

Now using Poisson's equation we obtain

$$\phi(\omega, k_x, y) = \frac{2}{\epsilon}\int_{-\infty}^{\infty} dy' K_0(|k_x||y - y'|)\rho(\omega, k_x, y'), \tag{9}$$

where $K_0(x)$ is the modified Bessel function; ϕ and ρ pertain to the 2D plane. From Eqs. (8) and (9) we obtain the following integral equation for $\rho(\omega, k_x, y)$:

$$-i(\omega - k_x v_g)\rho(\omega, k_x, y) + \frac{2}{\epsilon}\left\{k_x^2\sigma_{xx}(y) - ik_x\frac{d}{dy}[\sigma_{yx}^0(y)]\right.$$

$$\left. - \sigma_{yy}(y)\frac{d^2}{dy^2} - \frac{d}{dy}[\sigma_{yy}(y)]\frac{d}{dy}\right\}$$

$$\times \int_{-\infty}^{\infty} dy' K_0(|k_x||y - y'|)\rho(\omega, k_x, y') = 0. \tag{10}$$

The value of $\sigma_{yy}(y)$ is significantly different from zero only near the edges of the channel. The same holds for the values of $\sigma_{xx}(y)$ and of $d\sigma_{yx}^0(y)/dy$; for $\hbar v_g \gg \ell_0 k_B T$ this can be seen from Eqs. (4) and (6) which show that $\sigma_{yy}(y)$ and $d\sigma_{yx}^0(y)/dy$ are exponentially localized within a distance $\approx \ell_0$ from the right edge at $y_{re} = y_r + \Delta y_r$. We have $\Delta y_r = \ell_0^2 k_e$, where $k_e = (\omega_c/\hbar\Omega)\sqrt{2m^*\Delta_F}$ is the characteristic wave vector associated with an edge state, $\Delta_F = E_{F0} - \hbar\omega_c/2$, and $W = 2y_{re}$. For $k_{x\alpha} \equiv k_{re} = y_r/\ell_0^2 + k_e$, we have $f_0(k_{re}) = \frac{1}{2}$ and

$$v_g = \frac{1}{\hbar}\frac{\partial E_0(k_{re})}{\partial k_{x\alpha}} = \frac{\hbar\Omega^2 k_e}{m^*\omega_c^2} = \left(\frac{2\Delta_F}{m^*}\right)^{1/2}\frac{\Omega}{\omega_c}. \tag{11}$$

Equation (11) can also be written as $v_g = E_e/B$, where $E_e = \Omega\sqrt{2m^*\Delta_F}/|e|$ is the electric field describing the influence of the confining potential. For a dissipationless, 2D classical electron liquid we have, for finite ω, $\sigma_{yy}(y) = \sigma_{xx}(y) = ie^2 n_0(y)\omega/m^*(\omega^2 - \omega_c^2)$ and $\sigma_{yx}^0(y) = -e^2 n_0(y)\omega_c/m^*(\omega^2 - \omega_c^2)$, where n_0 is the electron density. Then Eq. (10) becomes identical with Eq. (4) of Ref. 11. In addition, if we assume that the conductivity components in Eq. (10) are independent of y, for $|y| < W/2$, and $\sigma_{yy}(y) = \sigma_{xx}(y)$, Eq. (10) takes the form of Eq. (15) of Ref. 1 after integration over z.

Equations (9) and (10) apply to a 2DEG in the absence of metallic gates. Sometimes a metallic gate is placed on the top of the sample[10] at a distance d from the 2DEG. As shown in the Appendix, for a gated sample the kernel K_0 in Eqs. (9) and (10) is replaced by $R_g = K_0(|k_x||y - y'|) - K_0(|k_x|\sqrt{(y - y')^2 + 4d^2})$. If this gate is replaced by air, then K_0 is replaced by $R_a = K_0(|k_x||y - y'|) + [(\epsilon - 1)/(\epsilon + 1)]K_0(|k_x|\sqrt{(y - y')^2 + 4d^2})$.

III. EMP DISPERSION RELATION

We consider very low temperatures that satisfy the inequality $\hbar v_g \gg \ell_0 k_B T$. From Eqs. (4) and (6) it follows that $d\sigma_{yx}^0(y)/dy = -(e^2/2\pi\hbar)\Psi_0^2(y - y_{re})$; also, $\sigma_{yy}(y)$ and $\sigma_{xx}(y)$ behave as $\Psi_0^2(y - y_{re})$, and hence are strongly concentrated near the edge. It follows from Eq. (10) that $\rho(\omega, k_x, y)$ is also concentrated near the edge. Integrating Eq. (10) over y, from $y_{re} - \Delta y$ to $y_{re} + \Delta y$ with $\Delta y \sim \ell_0$, we obtain

$$\int_{-\infty}^{\infty} dy \; \rho(\omega,k_x,y)\left[-(\omega-k_x v_g)\right.$$

$$\left. + S \int_{-\infty}^{\infty} dy' \Psi_0^2(y'-y_{\rm re})K_0(|k_x||y-y'|)\right]=0;$$

$$(12)$$

here $S=(2/\epsilon)(-ik_x^2\widetilde{\sigma}_{xx}+k_x\sigma_{yx}^0)$, $\sigma_{yx}^0=e^2/2\pi\hbar$ is the Hall conductivity in the bulk as follows from Eq. (4), and $\widetilde{\sigma}_{\mu\mu} = \sigma_{\mu\mu}(y)/\Psi_0^2[y-y_0(k_{\rm re})]$, $\mu=x$ and y. Using Eq. (6) for $v_g>s$ we obtain

$$\widetilde{\sigma}_{xx}\approx\widetilde{\sigma}_{yy}=\frac{3e^2\ell_0^4 c' k_B^3 T^3}{2\pi^2\hbar^6 v_g^4 s}.$$

$$(13)$$

Equation (13) coincides with $j_d W/E_y$, given by Eq. (32) of Ref. 13(a), for $E_y\rightarrow 0$. For $v_g<s$ the contribution to $\widetilde{\sigma}_{xx}$ is exponentially suppressed and has an activated behavior.[13] For $v_g^2\gg s^2$ we have $\widetilde{\sigma}_{xx}=e^2\ell_0^3 c' k_B^2 T^2/\sqrt{2}\pi^{5/2}\hbar^5 v_g^4$, if $1\gg k_B T\ell_0/\hbar v_g>s/\sqrt{2}v_g$, and Eq. (13) if $1\gg k_B T\ell_0/\hbar v_g<s/\sqrt{2}v_g$.

Notice that the terms in Eq. (10) related to $\sigma_{yy}(y)$ are totally absent in Eq. (12). Now, in Eq. (12) we have $|y-y'|\sim\ell_0$ and $|k_x|\ell_0\sim 10^{-6}$; then we can make the approximation $K_0(|k_x||y-y'|)\approx\ln(2/|k_x\ell_0|)-\gamma-\ln(|y-y'|/\ell_0)$, where γ is the Euler constant. The value of the integral over y' in Eq. (12) is $\ln(2/|k_x\ell_0|)-\gamma-(1/\sqrt{\pi})\int_{-\infty}^{\infty}dt\; e^{-t^2}\ln|t-(y-y_{\rm re})/\ell_0|$. For the gated sample and that with air above $z=d$, $4d^2\gg\ell_0^2$, the corresponding approximations in the long-wavelength limit are $R_g\approx\ln(2d/\ell_0)-\ln(|y-y'|/\ell_0)$ and, with $\epsilon\gg 1$, $R_a\approx\ln(2/k_x^2 d\ell_0)-2\gamma-\ln(|y-y'|/\ell_0)$, respectively.

Now for $T\rightarrow 0$ we have $\widetilde{\sigma}_{xx}\rightarrow 0$, $\widetilde{\sigma}_{yy}\rightarrow 0$, and Eq. (10) shows that $\rho(\omega,k_x,y)$ behaves essentially as $\Psi_0^2(y-y_{\rm re})$. Then the value related to the integral over t can be evaluated and gives a small contribution compared to that of the term $\ln(1/|k_x\ell_0|)$. The result is

$$\left\{-(\omega-k_x v_g)+S\left[\ln\frac{1}{|k_x\ell_0|}+\frac{3}{4}\right]\right\}\int_{-\infty}^{\infty}dy\;\rho(\omega,k_x,y)=0.$$

$$(14)$$

From Eq. (14) it follows that the EMP dispersion relation, with strong dissipation at the edges and for $k_B T\ll\hbar v_g/\ell_0$, is given by $[\omega(k_x)\equiv\omega]$

$$\omega=k_x v_g+\frac{2}{\epsilon}[k_x\sigma_{yx}^0-ik_x^2\widetilde{\sigma}_{xx}]\left[\ln\frac{1}{|k_x\ell_0|}+\frac{3}{4}\right].$$

$$(15)$$

For $\nu=2$ the EMP dispersion relation will again be given by Eq. (15), with the conductivity components multiplied by a factor of 2. In addition, because v_g has the $\sim 1/B$ dependence, cf. Eq. (11), it will be multiplied, for $\nu=2$, by a factor of 2 if the edge field E_e is the same. As a result, for $\nu=2$ the frequency ω will be approximately twice as large as for $\nu=1$. More exactly, the value of the ratio of these frequencies is

$$\frac{\omega(\nu=2)}{\omega(\nu=1)}=2\left\{1-\frac{\ln 2}{2[\ln(1/|k_x\ell_0|)+3/4]}\right\},\quad (16)$$

where ℓ_0 corresponds to $\nu=1$. For $k_x\ell_0\sim 10^{-6}$, the second term inside the curly brackets represents a 2% correction.

Equation (15) is valid for an ungated sample. If the sample is gated, repeating the procedure leads again to Eq. (15) with the factor [ ] replaced by $[\ln(2d/\ell_0)+2/\pi]$. If the gate is replaced by air, this factor is replaced by $[\ln(1/k_x^2 d\ell_0)]$.

IV. EDGE WAVES AT VERY LOW TEMPERATURES

From Eq. (10) it follows that, even for $T\rightarrow 0$, $\rho(\omega,k_x,y)=\rho^{(0)}(\omega,k_x)\Psi_0^2(\bar{y})$, where $\bar{y}=y-y_{\rm re}$, is only an approximate solution of this equation. A more accurate solution is obtained by the expansion

$$\rho(\omega,k_x,y)=\Psi_0^2(\bar{y})\sum_{n=0}^{\infty}\rho^{(n)}(\omega,k_x)H_n(\bar{y}/\ell_0)$$

$$=\sum_{n=0}^{\infty}\sqrt{2^n n!}\rho^{(n)}(\omega,k_x)\Psi_n(\bar{y})\Psi_0(\bar{y}),\quad (17)$$

where $H_n(x)$ are the Hermite polynomials. Due to their orthonormality Eq. (17) is the exact expression for $\rho(\omega,k_x,y)$. Notice that this expansion is specific to the case when only the lowest LL is occupied. In addition, the terms $n=0$, $n=1$, $n=2$, etc. correspond to the monopole, dipole, quadrupole, etc. expansions of $\rho(\omega,k_x,y)$ relative to $y=y_{\rm re}$.

We now multiply Eq. (10) by $H_m(\bar{y}/\ell_0)$ and integrate over y from $y_{\rm re}-\Delta y$ to $y_{\rm re}+\Delta y$. Taking into account that for very low temperatures $(\hbar v_g\gg\ell_0 k_B T)$ $d\sigma_{yx}^0(y)/dy$, $\sigma_{yy}(y)$, and $\sigma_{xx}(y)$ behave as $\Psi_0^2(\bar{y})$, we obtain

$$-(\omega-k_x v_g)\rho^{(m)}(\omega,k_x)+(S+mS')$$

$$\times\sum_{n=0}^{\infty}\left(\frac{2^n n!}{2^m m!}\right)^{1/2}a_{mn}(k_x)\rho^{(n)}(\omega,k_x)=0,\quad (18)$$

where

$$a_{mn}(k_x)=a_{nm}(k_x)=\int_{-\infty}^{\infty}dx\;\Psi_m(x)\Psi_0(x)$$

$$\times\int_{-\infty}^{\infty}dx'\;K_0(|k_x||x-x'|)\;\Psi_n(x')\Psi_0(x')$$

$$(19)$$

and $S'=-4i\widetilde{\sigma}_{yy}/\epsilon\ell_0^2$. Notice that for $m=0$ Eq. (18) is equivalent to Eq. (12) and, correspondingly, the terms related to $\widetilde{\sigma}_{yy}$ are absent. From Eqs. (17)–(19) it follows that there exist independent wave modes, spatially *symmetric*, $\rho^s(\omega,k_x,y)$, and *antisymmetric*, $\rho^{as}(\omega,k_x,y)$, with respect to $y=y_{\rm re}$. They are given by Eqs. (17) and (18) with n *even* and *odd*, respectively. Notice that in Eq. (19) due to the assumption $k_x\ell_0\ll 1$ we can write $K_0(|x|)\approx\ln(2/|x|)-\gamma$ for the ungated sample. For the gated sample we simply replace

the kernel K_0 in Eq. (19) by $R_g \approx \ln(2d/\ell_0) - \ln(|y - y'|/\ell_0)$, and for that with air by $R_a \approx \ln(2/k_x^2 d\ell_0) - 2\gamma - \ln(|y - y'|/\ell_0)$.

A. Symmetric modes

Considering only the term $n=0$ in the expression for $\rho^s(\omega, k_x, y)$, Eq. (18) for $m=0$ gives

$$[-(\omega - k_x v_g) + S a_{00}]\rho^{(0)}(\omega, k_x) = 0, \qquad (20)$$

where $a_{00}(k_x) = -\ln(|k_x|\ell_0) + 3/4$. With this value of $a_{00}(k_x)$ and $\rho^{(0)}(\omega, k_x) \neq 0$, Eq. (20) gives the dispersion relation (15). Because $\rho^s(\omega, k_x, y)$ behaves spatially as $\Psi_0^2(\bar{y})$ in this approximation, we will refer to it as the dispersion relation of the monopole EMP. For the sample with a gate we simply have to replace a_{00} by $a_{00}^g = [\ln(2d/\ell_0) + 2/\pi]$ in Eq. (20) and for that with air by $a_{00}^a = \ln(1/k_x^2\ell_0 d)$.

Corrections to Eq. (20) and further *symmetric* branches are obtained by keeping only the terms $n=0$ and 2 in the expression for $\rho^s(\omega, k_x, y)$, which gives

$$\rho^s(\omega, k_x, y) = \rho^{(0)}(\omega, k_x)\Psi_0^2(\bar{y})$$
$$+ 2\sqrt{2}\rho^{(2)}(\omega, k_x)\Psi_2(\bar{y})\Psi_0(\bar{y}). \quad (21)$$

From Eq. (18) for $m=0$ we obtain

$$[-(\omega - k_x v_g) + S a_{00}]\rho^{(0)}(\omega, k_x) + 2\sqrt{2}S a_{02}\rho^{(2)}(\omega, k_x) = 0, \qquad (22)$$

and, for $m=2$,

$$[-(\omega - k_x v_g) + (S + 2S')a_{22}]\rho^{(2)}(\omega, k_x)$$
$$+ [(S + 2S')/2\sqrt{2}]a_{02}\rho^{(0)}(\omega, k_x) = 0, \qquad (23)$$

where we write $a_{mn}(k_x) \equiv a_{mn}$ in order to simplify the notation. For a nontrivial solution of the system of Eqs. (22) and (23) the 2×2 determinant of the coefficients must vanish. This gives two branches $\omega_+^s(k_x)$ and $\omega_-^s(k_x)$. For $|k_x|\ell_0 \ll 1$ a numerical evaluation gives $a_{02} = -0.353$, $a_{22} = 0.250$, and $a_{02}^2 = 1/8$. All a_{mn} values remain the same for gated samples or those with air, except a_{00}, which changes as indicated above. If we neglect the coupling terms, by formally setting $a_{02}(k_x) = 0$, Eq. (22) gives the monopole EMP dispersion relation (15) and Eq. (23) the pure quadrupole EMP dispersion relation

$$\omega = k_x v_g + (S + 2S')/4$$
$$= k_x v_g + \frac{1}{2\epsilon}\left[k_x\sigma_{yx}^0 - ik_x^2\tilde{\sigma}_{xx} - 4i\frac{\tilde{\sigma}_{yy}}{\ell_0^2}\right]. \qquad (24)$$

If we neglect $k_x v_g$ and the dissipative terms, Eq. (24) takes the form of Eq. (14) of Ref. 11 for the $j=4$ branch, which has five charge oscillations. As it stands, Eq. (24) corresponds to only three oscillations. The difference is to be ascribed to the very different density profile used in Ref. 11 for a compressible liquid in a very wide strip. Notice that Eq. (24) is valid for samples with gate or air as well.

For finite a_{02} the two branches resulting from Eqs. (22) and (23) are given by

$$\omega_\pm^s = k_x v_g + \frac{1}{2}[S(a_{00} + a_{22}) + 2S'a_{22}]$$
$$\pm \frac{1}{2}\sqrt{[S(a_{00} - a_{22}) - 2S'a_{22}]^2 + 4S(S + 2S')a_{02}^2}. \qquad (25)$$

If we put $a_{02} = 0$, i.e., if we neglect the coupling between the branches, then the $\omega_-^s(k_x)$ branch is given by Eq. (24) and the $\omega_+^s(k_x)$ branch coincides with Eq. (15). It can be shown that the term $\propto a_{02}^2$ under the square root sign is much smaller than the other term. Then from Eq. (25) we obtain

$$\omega_+^s = k_x v_g + S a_{00} + \frac{S(S + 2S')a_{02}^2}{S a_{00} - (S + 2S')a_{22}} \qquad (26)$$

and

$$\omega_-^s = k_x v_g + (S + 2S')a_{22} - \frac{S(S + 2S')a_{02}^2}{S a_{00} - (S + 2S')a_{22}}. \qquad (27)$$

Further, for very low temperatures we can distinguish between (i) strong dissipation, for which $k_x\sigma_{yx}^0 \ll 4\tilde{\sigma}_{yy}/\ell_0^2$; and (ii) weak dissipation, for which $k_x\sigma_{yx}^0 \gg 4\tilde{\sigma}_{yy}/\ell_0^2$. Notice that the damping of the purely quadrupole EMP—Eq. (24)—is such that in case (i) we have $|\text{Im}\omega| \gg |\text{Re}\omega|$, whereas in case (ii) the opposite inequality holds. The damping of Eq. (24) is determined by the dissipative conductivities $\sigma_{yy}(y)$ and $\sigma_{xx}(y)$. The two contributions differ by a very small factor $k_x^2\ell_0^2$. As a result, the damping of the wave, $\propto k_x^2\tilde{\sigma}_{xx}$, can be usually neglected. Notice that Eqs. (22)–(27) are valid for gated or ''air'' samples as well, with a_{00} replaced by a_{00}^g or a_{00}^a.

For definiteness in numerical estimates, we will use parameters pertinent to GaAs/AsAl$_x$Ga$_{1-x}$As heterostructures. As will be shown below, both cases (i) and (ii) are experimentally realized depending on the values of v_g and T. For $v_g \lesssim s$ the damping in Eq. (24) is exponentially suppressed. The condition $v_g < s$ requires a smooth energy dispersion near the edges. This possibility exists in the Hartree approximation for the confining potential but not in the Hartree-Fock approximation, where the exchange leads to a logarithmically divergent[16] v_g. However, when correlations are taken into account, a smooth energy dispersion results near the edges and v_g is small.[16] In GaAs-based heterostructures, the most common case is $v_g > s = 2.5 \times 10^5$ cm/s. In this case using Eq. (13) for $\nu = 1$, $c' = \hbar(eh_{14})^2/2\rho_V s$, $h_{14} = 1.2 \times 10^7$ V/cm, and $\rho_V = 5.31$ gm/cm^3, we obtain

$$\frac{\tilde{\sigma}_{yy}}{\ell_0\sigma_{yx}^0} = 0.16\tilde{T}^3\tilde{B}^{-3/2}\tilde{v}_g^{-4}, \qquad (28)$$

where $\tilde{T} = T/1$ K, $\tilde{B} = B/(10$ T$)$, and $\tilde{v}_g = v_g/s$. Equation (28) is valid for $\nu = 2$ as well, because of the scaled quantities. For $\tilde{T} = 1$, $\tilde{B} = 1$, and $\tilde{v}_g = 2$, Eq. (28) gives $\tilde{\sigma}_{yy}/\ell_0\sigma_{yx}^0\tilde{\sigma}_{yy}/\ell_0\sigma_{yx}^0 = 10^{-2}$. The estimated[17] field E_e leads, for $\tilde{B} = 1$, to $v_g \approx 4 \times 10^5$cm/s $> s$. Further, if we assume that $\tilde{\sigma}_{yy}/\ell_0$ gives approximately the value of the diagonal conductivity in the edge strip of width $\ell_0 \approx 80$ Å, then, because for strong magnetic fields $(\omega_c\tau^* \gg 1)$

$\widetilde{\sigma}_{yy}/\ell_0\sigma_{yx}^0\approx1/\omega_c\tau^*=10^{-2}$, we obtain an effective scattering rate $1/\tau^*\approx\omega_c\widetilde{\sigma}_{yy}/\ell_0\sigma_{yx}^0\approx2.6\times10^{11}$/s in this strip. This is approximately ten times larger than the scattering rate for a mobility $\mu=10^6$ cm^2/V s.

From Eq. (24) we obtain

$$\frac{|\text{Re}\,\omega|}{|\text{Im}\,\omega|}\approx\frac{\sigma_{yx}^0|k_x|\ell_0}{4\widetilde{\sigma}_{yy}/\ell_0}\approx1.5\widetilde{T}^{-3}\widetilde{B}^{-3/2}\widetilde{v}_g^4|k_x|\ell_0, \quad (29)$$

where we assumed again that the term v_gk_x can be neglected. Then, for $\widetilde{T}=1,\widetilde{B}=1$, and $\widetilde{v}_g=2$, the right-hand side of Eq. (29) is approximately equal to $25|k_x|\ell_0$. Only for $1\gg|k_x|\ell_0>4\times10^{-2}$ does the quadrupole EMP become weakly dissipative. For $\widetilde{B}=1$, lower temperature $\widetilde{T}=0.1$, and steeper confinement $\widetilde{v}_g=4$, Eq. (29) gives $|\text{Re}\,\omega|/|\text{Im}\,\omega|\approx5\times10^5|k_x|\ell_0$. In this case the quadrupole wave is very weakly damped for 1.25×10^6 cm$^{-1}\gg|k_x|>2.5$ cm^{-1}. In this region the implicit low-frequency condition $|\omega|\ll\omega_c$ is well satisfied, since it corresponds to $|k_x|\ll1.6\times10^7$ cm^{-1}.

B. Edge helicons

We now analyze further the general formulas of Sec. IV A. We first assume that $\sigma_{yx}^0|k_x|K\gg\widetilde{\sigma}_{yy}/\ell_0^2$. Then Eq. (27) gives

$$\omega_-^s=k_xv_g+\tfrac{1}{4}(S+2S')\left(1-\frac{1}{2K}\right), \quad (30)$$

where $K=a_{00}-1/4=\ln(1/|k_x|\ell_0)+1/2$; for gated or ''air'' samples, a_{00} in K is replaced by a_{00}^g and a_{00}^a, respectively. Because $\ln(1/|k_x|\ell_0)\gg1$, we see that the coupling with the monopole EMP does not change the dispersion almost at all as compared with that given by Eq. (24). As a result the quasiquadrupole EMP, described by Eq. (30), is weakly damped for $\sigma_{yx}^0|k_x|>4\widetilde{\sigma}_{yy}/\ell_0^2$ and strongly damped for $4\widetilde{\sigma}_{yy}/\ell_0^2>\sigma_{yx}^0|k_x|\gg\widetilde{\sigma}_{yy}/\ell_0^2K$. We call the wave described by Eq. (30) a quasiquadrupole EMP because it follows from Eq. (23) that

$$\frac{\rho^{(2)}(\omega,k_x)}{\rho^{(0)}(\omega,k_x)}=-2\sqrt{2}a_{02}K=K\gg1; \quad (31)$$

that is, $\rho^{(2)}(\omega,k_x)$ is the dominant term on the right-hand side of Eq. (21). The same holds for the ''air'' sample. However, for the gated sample the monopole and quadrupole terms are comparable if $K_g\lesssim3$. The condition of very weak damping for the wave (30) can also be expressed as $\omega_-^s\tau^*\gg\nu r_0/\pi$, where $r_0=e^2/\epsilon\hbar\omega_c\ell_0$. For $\nu=1$ we typically have $r_0\sim1$. This condition resembles the high-frequency limit used in Ref. 1. However, here τ^* is related to dissipation processes only near the edge. In addition, in contrast with Ref. 1, we consider an essential decrease of the conductivity components and of the electron density over a finite length Λ_y from the edge. For very low temperatures, $k_BT\ll\hbar v_g/\ell_0$, we have $\Lambda_y\approx\ell_0$, which is much smaller than the length over which the density $n_0(y)$ decreases substantially in the model of Ref. 11.

For $\sigma_{yx}^0|k_x|K\gg\widetilde{\sigma}_{yy}/\ell_0^2$, Eq. (26) gives

$$\omega_+^s=k_xv_g+S(K+1/4)\left[1+\frac{1}{8K(K+1/4)}\right]+\frac{S'}{4K}. \quad (32)$$

As can be seen, taking into account the coupling with the quadrupole EMP changes the phase velocity of the monopole EMP by a very small amount ($\lesssim0.1\%$) but it makes an important new contribution to the damping in comparison with Eq. (15). Now the ω_+^s branch, for the typical EMP condition $|k_x|\ell_0\sim10^{-6}$, has a damping $\propto\widetilde{\sigma}_{yy}/\ell_0^2K$ which is much stronger than that $\propto\widetilde{\sigma}_{xx}k_x^2K$ of the pure monopole EMP.

The wave described by Eq. (32) can be called a quasimonopole EMP because it follows from Eq. (22) that

$$\frac{\rho^{(0)}(\omega,k_x)}{\rho^{(2)}(\omega,k_x)}=\frac{16\sqrt{2}a_{02}\sigma_{yx}^0k_xK}{\sigma_{yx}^0k_x-4i\widetilde{\sigma}_{yy}/\ell_0^2}, \quad (33)$$

and, due to $K\gg1$, we have $|\rho^{(0)}(\omega,k_x)/\rho^{(2)}(\omega,k_x)|\gg1$. Now, for weak dissipation ($\sigma_{yx}^0k_x\gg4\widetilde{\sigma}_{yy}/\ell_0^2$) we have $\rho^{(0)}(\omega,k_x)/\rho^{(2)}(\omega,k_x)\approx-8K$ and for strong dissipation ($\sigma_{yx}^0k_xK\gg\widetilde{\sigma}_{yy}/\ell_0^2\gg\sigma_{yx}^0k_x/4$) $\rho^{(0)}(\omega,k_x)/\rho^{(2)}(\omega,k_x)\approx-2i(\sigma_{yx}^0k_x\ell_0^2/\widetilde{\sigma}_{yy})K$. Thus, if the phases of the two components are shifted by π in the first case, in which we call the ω_+^s branch described by Eq. (32) a modified monopole EMP (MMEMP), they are shifted by $\pi/2$ in the last one. This last case corresponds to the frequency region $\omega_+^s\tau^*\gg\nu r_0/\pi\gg[\omega_+^s\tau^*/(4K+1)]$, and the frequency ω_+^s can still be considered as high compared to $1/\tau^*$. In this frequency region we call the ω_+^s branch the high-frequency *edge helicon* (HFEH) and denote it by $\omega_{\text{EH}}^{\text{HF}}$. In this region, due to the almost $\pi/2$ shift between $\rho^{(0)}$ and $\rho^{(2)}$, we obtain the following remarkable property of HFEH described by Eq. (32). If the HFEH charge $\propto\text{Re}\{\rho^s(\omega_{\text{EH}}^{\text{HF}},k_x,y)R_+(x,t)\}$ along y has a pure quadrupole character $\propto|\rho^{(2)}|$ for some phase of the running wave $R_+(x,t)=\exp[-i(\omega_{\text{EH}}^{\text{HF}}t-k_xx)]$, then after approximately a $\pm\pi/2$ shift it acquires a pure monopole character $\propto|\rho^{(0)}|$; $\rho^s(\omega_{\text{EH}}^{\text{HF}},k_x,y)$ is given by Eq. (21). This HFEH shows *three* charge oscillations along y whereas the relevant branches of Refs. 1 and 11 with $\text{Re}\,\omega\propto k_x\ln(1/k_x)$ resembling $\text{Re}\,\omega_{\text{EH}}^{\text{HF}}$ of the HFEH, show only *one* oscillation.

Notice that $\text{Re}\,\omega_+^s$, given by Eq. (32) is independent of T whereas $\text{Im}\,\omega_+^s\propto T^3$ or T^2 if $1\gg k_BT\ell_0/\hbar v_g\gg s/\sqrt{2}v_g$. That is, in contrast with Ref. 1, we find that the damping of the MMEMP and that of the HFEH scale with temperature and are not quantized in the QHE plateaus. In addition, these waves have a characteristic length ℓ_0 which is different than the length ℓ_v of Ref. 1; also, the term $\propto\sigma_{yx}^0$ is different than that of Ref. 1 in the factor containing the logarithm. In addition, $\ell_0(\nu=2)/\ell_0(\nu=1)=\sqrt{2}$ here whereas $\ell_v(\nu=2)/\ell_v(\nu=1)=4$ in the high-frequency limit of Ref. 1. Moreover, for $\epsilon\to\infty$ it follows that $\ell_v(\nu=1)\to0$ whereas ℓ_0 is independent of ϵ.

We now consider the case of very strong dissipation,

$$\widetilde{\sigma}_{yy}/\ell_0^2\gg\sigma_{yx}^0|k_x|K. \quad (34)$$

Then Eq. (27) gives

$$\omega_-^s = k_x v_g + \frac{1}{2\epsilon} \left[3\sigma_{yx}^0 k_x - 4i\widetilde{\sigma}_{yy}/\ell_0^2\right]. \qquad (35)$$

This is again a quasiquadrupole wave, since $|\rho^{(2)}(\omega, k_x)/\rho^{(0)}(\omega, k_x)| \approx \widetilde{\sigma}_{yy}/\sigma_{yx}^0 |k_x| \ell_0^2 \gg 1$. Also, although $\mathrm{Re}\,\omega_-^s/k_x$ is essentially larger than in Eq. (30), Eq. (34) gives an *aperiodic damping*, $|\mathrm{Re}\,\omega_-^s| \ll |\mathrm{Im}\,\omega_-^s|$. Further, assuming that Eq. (34) is valid, we obtain from Eq. (26) the dispersion relation of a wave that we call a low-frequency *edge helicon* (LFEH),

$$\omega_{\mathrm{EH}}^{\mathrm{LF}} = k_x v_g + S(K - \tfrac{1}{4}) - \frac{i}{\epsilon} \frac{[\sigma_{yx}^0 k_x]^2}{\widetilde{\sigma}_{yy}/\ell_0^2}(K - \tfrac{1}{4}). \qquad (36)$$

Despite the strong dissipation condition (34), which entails $\omega_{\mathrm{EH}}^{\mathrm{LF}} \tau^* \ll \nu r_0/\pi \lesssim 1$, the LFEH is very weakly damped since $|\mathrm{Re}\,\omega_{\mathrm{EH}}^{\mathrm{LF}}| \gg |\mathrm{Im}\,\omega_{\mathrm{EH}}^{\mathrm{LF}}|$. The frequency range of the LFEH is similar to the low-frequency limit of Ref. 1, but here τ^* is related to strong dissipation processes only near the edges. Also, $\mathrm{Re}\,\omega_{\mathrm{EH}}^{\mathrm{LF}}/k_x$ differs little from $\mathrm{Re}\,\omega_{\mathrm{EH}}^{\mathrm{HF}}/k_x$ or that of Eq. (15). However, the damping of the LFEH $\propto (\sigma_{yx}^0 k_x \ell_0)^2 \ln(1/k_x \ell_0)/\widetilde{\sigma}_{yy}$ has a very different form than $\mathrm{Im}\,\omega_{\mathrm{EH}}^{\mathrm{HF}}$ of Eq. (32) or $\mathrm{Im}\,\omega$ of Eq. (15).

We further notice that, in contrast to Ref. 1, the real part $\mathrm{Re}\,\omega_{\mathrm{EH}}^{\mathrm{LF}}$ is independent of temperature whereas the imaginary part $\mathrm{Im}\,\omega_{\mathrm{EH}}^{\mathrm{LF}}$, i.e., the damping, is not quantized and varies as T^{-3} or T^{-2}; the T^{-2} behavior occurs if $v_g^2 \gg s^2$ and $1 \gg k_B T \ell_0/\hbar v_g \gg s/\sqrt{2}v_g$. That is, the LFEH has a characteristic length very different than ℓ_v in the low-frequency limit. It follows from Eq. (22) that

$$\frac{\rho^{(0)}(\omega_{\mathrm{EH}}^{\mathrm{LF}}, k_x)}{\rho^{(2)}(\omega_{\mathrm{EH}}^{\mathrm{LF}}, k_x)} \approx -4\sqrt{2}a_{02} = 2. \qquad (37)$$

With this result and Eq. (21), we obtain the dimensionless charge density profile of the LFEH, $\widetilde{\rho}_{\mathrm{EH}}(y) = \sqrt{\pi}\ell_0 \rho^s(\omega_{\mathrm{EH}}^{\mathrm{LF}}, k_x, y)/\rho^{(0)}(\omega_{\mathrm{EH}}^{\mathrm{LF}}, k_x)$, as

$$\widetilde{\rho}_{\mathrm{EH}}(y) = \sqrt{\pi}\ell_0 [\Psi_0^2(\bar{y}) + \sqrt{2}\Psi_2(\bar{y})\Psi_0(\bar{y})]. \qquad (38)$$

In Fig. 2 we show $\widetilde{\rho}_{\mathrm{EH}}(y)$ (solid curve), its monopole component (term $\propto \Psi_0^2$, short-dashed curve), and its quadrupole component (term $\propto \Psi_0\Psi_2$, long-dashed curve). For contrast, the dotted curve represents the normalized unperturbed electron density $n_0(y)/n_0$. As can be seen the monopole and quadrupole contributions are of the same order of magnitude, and the resultant $\widetilde{\rho}_{\mathrm{EH}}(y)$ has an oscillatory behavior with two oscillations, one to the right and one to the left of the edge at $y = y_{\mathrm{re}}$. This is in sharp contrast with the "usual" EMPs of Ref. 1, and the $j = 0$ mode of Ref. 11.

C. Antisymmetric modes

Considering only the term $n = 1$ in the expression for $\rho^{as}(\omega, k_x, y)$, and using Eq. (18) for $m = 1$, we obtain

$$[-(\omega - k_x v_g) + (S + S')a_{11}]\rho^{(1)}(\omega, k_x) = 0; \qquad (39)$$
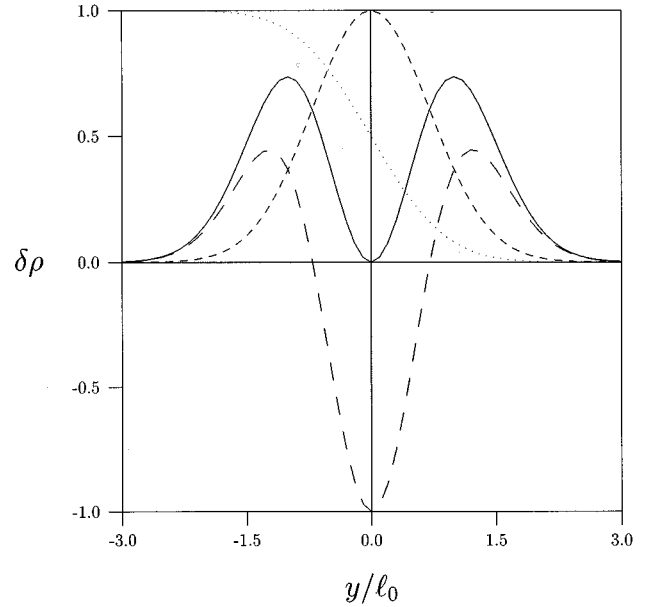

FIG. 2. Dimensionless charge density profile $\widetilde{\rho}_{\mathrm{EH}}(y)$ of the low-frequency edge helicon (LFEH) described by Eq. (38) as a function of $\bar{y}/\ell_0$ (solid curve). The dotted curve represents $n_0(y)/n_0$. The dashed and long-dashed curves are the pure monopole and quadrupole contributions, respectively. The oscillatory behavior of $\widetilde{\rho}_{\mathrm{EH}}(y)$ near the edge is in sharp contrast with the "usual" EMP of Refs. 1 and 11.

the numerically obtained value of a_{11} is 0.5. For $\rho^{(1)}(\omega, k_x) \neq 0$ Eq. (39) gives the dispersion relation of the pure dipole EMP as

$$\omega = k_x v_g + (1/\epsilon)[k_x \sigma_{yx}^0 - 2i\widetilde{\sigma}_{yy}/\ell_0^2]. \qquad (40)$$

If we neglect $k_x v_g$ and the dissipative term, Eq. (40) will take the form of Eq. (14) of Ref. 11 for $j = 2$, which shows three charge oscillations, whereas Eq. (40) corresponds to only two oscillations. However, in contrast to Ref. 11, besides the term $k_x v_g$ and the microscopically treated dissipative term, the Hall conductivity σ_{yx}^0 is quantized for $\nu = 1$ or 2.

Corrections to Eqs. (39) and (40), and further antisymmetric branches, are obtained by keeping only the $n = 1$ and $n = 3$ terms in the expression for $\rho^{as}(\omega, k_x, y)$. Then

$$\rho^{as}(\omega, k_x, y) = \sqrt{2}\rho^{(1)}(\omega, k_x)\Psi_1(\bar{y})\Psi_0(\bar{y})$$
$$+ 4\sqrt{3}\rho^{(3)}(\omega, k_x)\Psi_3(\bar{y})\Psi_0(\bar{y}). \qquad (41)$$

From Eqs. (18) and (19), for $m = 1$, we obtain

$$[-(\omega - k_x v_g) + (S + S')a_{11}]\rho^{(1)}(\omega, k_x)$$
$$+ 2\sqrt{6}(S + S')a_{13}\rho^{(3)}(\omega, k_x) = 0, \qquad (42)$$

and, for $m = 3$,

$$[-(\omega-k_x v_g)+(S+3S')a_{33}]\rho^{(3)}(\omega,k_x)$$

$$+(1/2\sqrt{6})(S+3S')a_{13}\rho^{(1)}(\omega,k_x)=0. \qquad (43)$$

Again the vanishing of the 2×2 determinant of the coefficients gives the two branches ω_-^{as} and ω_+^{as}. In the long-wavelength limit we numerically evaluate $a_{13}=-0.204$ and $a_{33}=0.166=\frac{1}{6}$. If we neglect the coupling between the modes, by formally setting $a_{13}=0$, Eq. (42) gives the disper-

sion relation for the pure dipole EMP, Eq. (40), and Eq. (43) that for the octupole EMP,

$$\omega=k_x v_g+(1/3\epsilon)[k_x\sigma_{yx}^0-6i\widetilde{\sigma}_{yy}/\ell_0^2]. \qquad (44)$$

If we neglect $k_x v_g$ and the dissipative term, Eq. (44) takes the form of Eq. (14) of Ref. 11 for the $j=6$ branch that shows seven charge oscillations. As it stands, Eq. (44) corresponds only to four charge oscillations.

For finite a_{13} the two branches resulting from Eqs. (42) and (43) are given by

$$\omega_\pm^{as}=k_x v_g+\tfrac{1}{2}[S(a_{11}+a_{33})+S'(a_{11}+3a_{33})]\pm\tfrac{1}{2}\sqrt{[S(a_{11}-a_{33})+S'(a_{11}-3a_{33})]^2+4a_{13}^2(S+S')(S+3S')}. \qquad (45)$$

If we set $a_{13}=0$, ω_+^{as} and ω_-^{as} give the dipole and octupole branches given above by Eqs. (40) and (44), respectively. For weak dissipation we have $k_x\sigma_{yx}^0\gg4\widetilde{\sigma}_{yy}/\ell_0^2$, and, if we neglect damping, we obtain

$$\omega_+^{as}\approx k_x v_g+(6/5\epsilon)\sigma_{yx}^0 k_x \qquad (46)$$

and

$$\omega_-^{as}\approx k_x v_g+(1/7\epsilon)\sigma_{yx}^0 k_x. \qquad (47)$$

We call the waves corresponding to Eqs. (46) and (47) modified dipole (MDEMP) and octupole (MOEMP) EMP's, respectively. As we now show, some of their properties are essentially different than those of the pure dipole [Eq. (40)] and octupole [Eq. (44)] EMP's.

Then from Eq. (42) for the MDEMP, we calculate

$$\frac{\rho^{(1)}(\omega,k_x)}{\rho^{(3)}(\omega,k_x)}=20\sqrt{6}a_{13}=-10.0. \qquad (48)$$

With this ratio and Eq. (41) the dimensionless charge-density profile $\widetilde{\rho}_\pm^{as}(\omega_\pm^{as},k_x,y)=\sqrt{\pi}\ell_0\rho^{as}(\omega_\pm^{as},k_x,y)/\rho^{(1)}(\omega_\pm^{as},k_x,y)$ of the MDEMP takes the form

$$\widetilde{\rho}_{MD}(y)\equiv\widetilde{\rho}_+^{as}(y)=\sqrt{2\pi}\ell_0[\Psi_1(\bar{y})\Psi_0(\bar{y})$$

$$-\tfrac{1}{2}\Psi_3(\bar{y})\Psi_0(\bar{y})]. \qquad (49)$$

In Fig. 3 we show $\widetilde{\rho}_{MD}(y)$ (solid curve), its dipole component [term $\propto\Psi_1(\bar{y})\Psi_0(\bar{y})$, short-dashed curve], and its octupole component [term $\propto\Psi_3(\bar{y})\Psi_0(\bar{y})$ long-dashed curve]. Again the dotted curve represents the normalized unperturbed electron density $n_0(y)/n_0$. As can be seen, the dipole and octupole contributions to $\widetilde{\rho}_{MD}(y)$ are of the same order of magnitude, though $\omega_+^{as}\equiv\omega_{MD}$, given by Eq. (46), is a bit different ($<20\%$) than $\mathrm{Re}\,\omega$ of the pure dipole EMP given by Eq. (40). As seen in Fig. 3, the MDEMP has four charge oscillations, whereas the dipole EMP has two. Thus, the corresponding density profiles are qualitatively different although the phase velocities are close to each other.

For the MOEMP, given by Eq. (47), we calculate, from Eq. (43),

$$\frac{\rho^{(3)}(\omega,k_x)}{\rho^{(1)}(\omega,k_x)}=2.109/2\sqrt{6}\approx1/\sqrt{6}; \qquad (50)$$

the corresponding result for $\widetilde{\rho}_{MO}(y)\equiv\widetilde{\rho}_-^{as}(y)$ is

$$\widetilde{\rho}_{MO}(y)=\sqrt{2\pi}\ell_0[\Psi_1(\bar{y})\Psi_0(\bar{y})+2\Psi_3(\bar{y})\Psi_0(\bar{y})]. \qquad (51)$$

In Fig. 4 we plot the same quantities as in Fig. 3 but now for $\widetilde{\rho}_{MO}(y)$. As can be seen, the spatial behavior of $\widetilde{\rho}_{MO}(y)$ is quantitatively different only than that of the pure octupole EMP. The phase velocities of these two EMP's, as follow from the dispersion relations, are substantially different. Notice that for strong dissipation, $k_x\sigma_{yx}^0\ll4\widetilde{\sigma}_{yy}/\ell_0^2$, both $\omega_\pm^{as}$ branches are strongly damped.
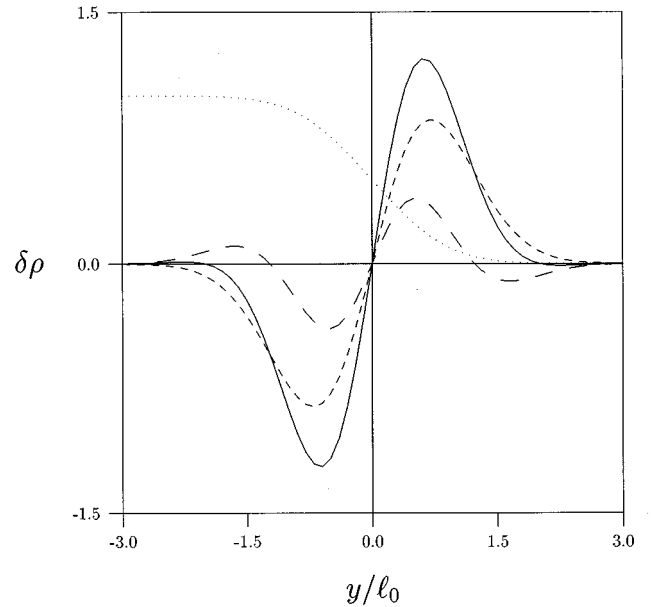

FIG. 3. Dimensionless charge-density profile $\widetilde{\rho}_{MD}(y)$ of the MDEMP described by Eq. (49) as a function of $\bar{y}/\ell_0$ (solid curve). The dashed and long-dashed curves are the pure dipole and octupole contributions, respectively. The dotted curve represents $n_0(y)/n_0$.
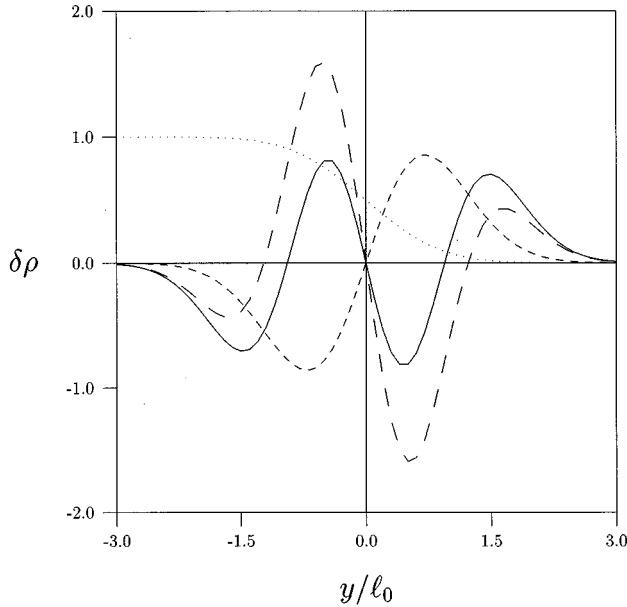
FIG. 4. As in Fig. 3, but for $\tilde{\rho}_{MO}(y)$ as described by Eq. (51).

V. DISCUSSION AND CONCLUDING REMARKS

We have introduced a realistic model for the confining potential $V_c(y)$, and treated mainly the case where $\nu=1$ in the interior part of the channel and the formation of dipolar strips[18] near the edges is impossible in the assumed QHE regime. We have taken $V_c(y)$ sufficiently steep at the edge that LL flattening can be neglected.[18–20] As for $\nu=2$, we neglected the spin splitting. This is a reasonable approximation in the bulk of the channel but its validity near the edges is not clear in view of the work of Refs. 16 and 21. Though we have used a simple form for $V_c(y)$, near the edge, the results remain valid for potentials $V_c(y)$ of different form that are smooth on the scale of ℓ_0. In such a case, e.g., the last term on the right-hand side of Eq. (5) should be replaced by $V_c(y_{0\alpha})$, and v_g will be given again by Eq. (11), with k_{re} determined by $f_0(k_{re})=\frac{1}{2}$. Thus v_g is the only parameter related to the form of V_c that influences these edge waves.

For a comparison of the theory with the experiment, the details of the sample geometry are necessary, but often they are not given. For instance, the thickness d_s of the sample is not given in Ref. 6; it is also not given neither in Ref. 22, where the bottom of the sample is metallized, nor in Ref. 9. Now concerning Ref. 5 it can be seen that $d_s=400$ μm for the sample with perimeter $P=1.7$ cm, and the observations were made at $T=0.4$ K and $B=13$ T ($\nu=1$). As we now show, the first three edge helicon modes $k_{x0}=2\pi/P$, $k_{x1}=2k_{x0}$, and $k_{x2}=3k_{x0}$ do not lead to an equidistant spectrum. Indeed, in addition to the case of the sample with air treated above, there is air for $z<-d_s$ (a foam plastic base with small dielectric constant). Then for $2k_xd_s\ll1$ we arrive at Eq. (9) with $\epsilon\approx1$, cf. Ref. 23, which should be substituted in all formulas involving a homogeneous ϵ; for $2k_xd_s\gg1$ we obtain the case of the ''air'' sample treated above. Taking into account that $2k_{x0}d_s=4\pi d_s/P\sim0.3$, $2k_{x1}d_s\sim0.6$, and $2k_{x2}d_s\sim0.9$, we can explain qualitatively the observed, not equidistant spectrum. A quantitative comparison is impos-

sible because the condition $|k_x|W\gg1$ is not satisfied ($|k_x|W\sim1$).

The sample of Ref. 8 is a circular mesa with diameter $D=540$ μm and height ~1 μm, in the middle of a wide GaAs/Al$_x$Ga$_{1-x}$As chip with thickness $d_s=500$ μm. The condition $2|k_x|d_s\gg1$ is well satisfied even for $k_{x0}=2/D=37$ cm^{-1}; the minimum value of k_x, k_{xmin}, involved in the experiment satisfies $k_{xmin}\gg k_{x0}$. As a result, the conditions $2k_{xmin}d_s\gg1$ and $k_{xmin}W\gg1$ are well satisfied as well. Because the square ''pulser'' gate, of width $L_p=10$ μm, was much smaller than the circumference πD, the initial charge distribution can be assumed to have a rectangular form, and therefore to have an essential contribution from the $k_{xn}=\pm nk_{x0}$, $n=1,2,\ldots$, modes distributed in the interval $k_{x0}\leq|k_{xn}|<\pi/L_p$. It is natural to assume that the typical $k_{xt}=|k_{xnt}|\approx\pi/2L_p$; for a rectangular form of the charge distortion along x, we have approximately a 50% contribution to the total spectral density for $|k_{xn}|\leq k_{xt}$. The model of the ''air'' sample, described briefly in the Appendix, fits perfectly to the experiment.[8] The distance d at which the 2DEG is situated beneath the surface is not given but from the mesa height it can be estimated to be $d\approx1000$ Å. This gives $K_a(k_{xt})\approx10.5$ for $B=5.1$ T. Further, assuming $\tilde{v}_g=2$, i.e., $v_g=5\times10^5$ cm/s, using $\tilde{B}=0.51$, $\tilde{T}=0.3$, and $\nu=1$, in the middle of a wide chip, obtained from the parameters of the experiment, and using Eq. (28), we obtain $\tilde{\sigma}_{yy}/\ell_0\sigma_{yx}^0\approx7.5\times10^{-4}$. It follows that $k_{xt}\ell_0K_a(k_{xt})\approx1.6\times10^{-2}\gg\tilde{\sigma}_{yy}/\ell_0\sigma_{yx}^0$ which corresponds to the first condition treated in Sec. IV B.

Notice that here $k_{xt}\ell_0\approx1.5\times10^{-3}<4\tilde{\sigma}_{yy}/\ell_0\sigma_{yx}^0\approx3\times10^{-3}$, i.e., we are dealing with the case of strong dissipation as detailed after Eq. (27). It follows that all modes, apart from the HFEH, are strongly damped. For instance, both the pure dipole [Eq. (40)] and quasiquadrupole [Eq. (30)] modes have Im$\omega\approx3.4\times10^{10}$/s which is a very large value compared to the damping rate of the experiment Im$\omega\approx2\times10^8$/s for $\nu=1$. Moreover, during the observed period for the travel around the edge $T_e\approx3.5\times10^{-9}$ sec the amplitude of the quasiquadrupole EMP or dipole EMP should practically vanish due to the exponentially small factor $<\exp(-100)$. We are left with the high-frequency edge helicons described by Eqs. (32) and (33). Equation (32) gives a decay rate Im$\omega_{EH}^{HF}\approx1.9\times10^8$/s which is in good agreement with the observations.[8] The corresponding group velocity for the HFEH, obtained from Eq. (32), is $v_g(k_{xt})\approx(2/\epsilon)\sigma_{yx}^0[\ln(1/k_{xt}\ell_0d)-2]$, and gives a period $T=\pi D/v_g(k_{xt})\approx3.4\times10^{-9}$/s which is in excellent agreement with the experimental value. Because after the first trip the pulse became 700 ps wider, we can estimate the range of Δk_x, around k_{xt}, which gives the most essential contribution to the pulse. Subtracting $v_g(k_{xt}+\Delta k_x/2)$ from $v_g(k_{xt}-\Delta k_x/2)$ leads, after some calculations, to $\Delta k_x/2k_{xt}\approx0.4$. This then gives approximately $k_{xmax}=1.4k_{xt}$ and $k_{xmin}=0.6k_{xt}$.

Another important ingredient of our theory is the calculated damping rates. As shown above, they agree well with the observed rates.[8] The effective τ^* for the work of Ref. 8 is approximately 2.5×10^{-11} s. This is several decades shorter than that extracted from QHE measurements, which

is of the order of 10^{-3} s.[24] The difference is to be ascribed to the fact that in our model the dissipation is localized near the edges, whereas in that of Ref. 1 the dissipation occurs throughout the channel homogeneously. The latter is a reasonable assumption for relatively high temperatures, which have not been considered in the present work.

The results of Sec. IV have been obtained by considering only two terms, even or odd, in the sum over n in Eq. (17). Retaining further terms leads to somewhat wider but still oscillatory charge-density profiles. The resulting phase velocities of the HFEH and LFEH are nearly unchanged and the qualitative behavior of their damping rates is not affected.

Finally, it is worth noting that in our microscopically calculated dispersion relations the quantized Hall conductivity $\sigma_{yx} \equiv \sigma_{yx}^0$ appears explicitly. Though not shown here graphically, this accounts for the existence of plateaus in the transit times of the signals, as a function of magnetic field, observed recently in Ref. 22 and accounted for with the replacement of the quantity $e^2 n_0 / m^* \omega_c$) by the experimentally determined σ_{yx}. The present theory holds when only the $n=0$ LL is occupied. The coupling between edge excitations of different LL's will certainly affect the EMP modes presented here, and an appropriate extension of the theory is being planned.

ACKNOWLEDGMENTS

APPENDIX

As a model of a gated sample, we consider a 2DEG at $z=0$ with a metallic gate placed at a distance $z=d$ away from it and with a dielectric constant ϵ for $z<d$. Taking the Fourier transform, for $z<d$, with respect to x, y, and t, of Poisson's equation for the time-dependent charge density $\rho(x,y,z,t)$ gives

$$\epsilon \left[k^2 - \frac{\partial^2}{\partial z^2} \right] \phi(\omega,k_x,k_y,z) = 4\pi \rho(\omega,k_x,k_y)\delta(z),$$

$$(A1)$$

where $k^2 = k_x^2 + k_y^2$. For $z \leq 0$ we have

$$\phi_-(\omega,k_x,k_y,z) = A(\omega,k_x,k_y)\ e^{kz}, \qquad (A2)$$

and, for $0 \leq z < d$,

$$\phi_+(\omega,k_x,k_y,z) = B(\omega,k_x,k_y)e^{kz} + C(\omega,k_x,k_y)\ e^{-kz}. \qquad (A3)$$

Two boundary conditions are $\phi_+(\omega,k_x,k_y,d)=0$ and $\phi_+(\omega,k_x,k_y,+0)=\phi_-(\omega,k_x,k_y,-0)$. Integrating Eq. (A1) from $z=-0$ to $z=+0$ gives the third condition

$$\epsilon \left[\frac{\partial \phi_+(\omega,k_x,k_y,z)}{\partial z} \bigg|_{z=+0} - \frac{\partial \phi_-(\omega,k_x,k_y,z)}{\partial z} \bigg|_{z=-0} \right]$$

$$= -4\pi \rho(\omega,k_x,k_y). \qquad (A4)$$

From Eqs. (A2)–(A4) and the first two conditions, we obtain

$$\phi(\omega,k_x,k_y,z=0) = 2\pi \rho(\omega,k_x,k_y)(1 - e^{-2kd})/\epsilon k, \qquad (A5)$$

which gives

$$\phi(\omega,k_x,y) = \frac{1}{2\pi} \int_{-\infty}^{\infty} e^{ik_y y} \phi(\omega,k_x,k_y,z=0)dk_y$$

$$= \frac{2}{\epsilon} \int_{-\infty}^{\infty} \{ K_0(|k_x||y-y'|)$$

$$- K_0[|k_x|\sqrt{(y-y')^2 + 4d^2}] \} \rho(\omega,k_x,y')\ dy'.$$

$$(A6)$$

Notice that, for $d \to \infty$, Eq. (A6) coincides with Eq. (9).

If the gate is replaced by air, for $z>d$, a similar calculation leads again to Eq. (A6), with the kernel replaced by $R_a = K_0(|k_x||y-y'|) + [(\epsilon-1)/(\epsilon+1)]K_0[|k_x|\sqrt{(y-y')^2 + 4d^2}]$.

[1] V. A. Volkov and S. A. Mikhailov, Zh. Éksp. Teor. Fiz. **94**, 217 (1988) [Sov. Phys. JETP **67**, 1639 (1988)].

[2] D. B. Mast, A. J. Dahm, and A. L. Fetter, Phys. Rev. Lett. **54**, 1706 (1985).

[3] D-C. Glattli, E. Y. Andrei, G. Deville, J. Poitrenaud, and F. I. B. Williams, Phys. Rev. Lett. **54**, 1710 (1985).

[4] A. L. Fetter, Phys. Rev. B **33**, 3717 (1986).

[5] V. I. Tal'yanskii, I. E. Batov, B. K. Medvedev, J. P. Kotthaus, M. Wassermeier, A. Wixforth, J. Weimann, W. Schlapp, and H. Nikel, Pis'ma Zh. Éksp. Teor. Fiz. **50**, 196 (1989) [JETP Lett. **50**, 221 (1989)].

[6] M. Wassermeier, J. Oshinowo, J. P. Kotthaus, A. H. MacDonald, C. T. Foxon, and J. J. Harris, Phys. Rev. B **41**, 10 287 (1990).

[7] I. Grodnensky, D. Heitmann, and K. von Klitzing, Phys. Rev. Lett. **67**, 1019 (1991); Surf. Sci. **263**, 467 (1992).

[8] R. C. Ashoori, H. L. Stormer, L. N. Pfeiffer, K. W. Baldwin, and K. West, Phys. Rev. B **45**, 3894 (1992).

[9] V. I. Tal'yanskii, A. V. Polisski, D. D. Arnone, M. Pepper, C. G. Smith, D. A. Ritchie, J. E. Frost, and G. A. C. Jones, Phys. Rev. B **46**, 12 427 (1992).

[10] N. B. Zhitenev, R. J. Haug, K. v. Klitzing, and K. Eberl, Phys. Rev. Lett. **71**, 2292 (1993); Phys. Rev. B **49**, 7809 (1994).

[11] I. L. Aleiner and L. I. Glazman, Phys. Rev. Lett. **72**, 2935 (1994).

[12] S. Giovanazzi, L. Pitaevskii, and S. Stringari, Phys. Rev. Lett. **72**, 3230 (1994).

[13] O. G. Balev and P. Vasilopoulos, (a) Phys. Rev. B **47**, 16 410

(1993); (b)**50**, 8706 (1994); (c) **50**, 8727 (1994).

[14] O. G. Balev and P. Vasilopoulos, Phys. Rev. B **54**, 4863 (1996).

[15] L. D. Landau and E. M. Lifshitz, *Electrodynamics of Continuous Media* (Addison-Wesley, Reading, MA 1960).

[16] O. G. Balev and P. Vasilopoulos, Phys. Rev. B **56**, 6756 (1997).

[17] G. Muller, D. Weiss, A. V. Khaetskii, K. von Klitzing, S. Koch, H. Nickel, W. Schlapp, and R. Losch, Phys. Rev. B **45**, 3932 (1992).

[18] D. B. Chklovskii, B. I. Shklovskii, and L. I. Glazman, Phys. Rev. B **46**, 4026 (1992).

[19] T. Suzuki and T. Ando, J. Phys. Soc. Jpn. **62**, 2986 (1993).

[20] L. Brey, J. J. Palacios, and C. Tejedor, Phys. Rev. B **47**, 13 884 (1993).

[21] J. Dempsey, B. Y. Gelphand, and B. I. Halperin, Phys. Rev. Lett. **70**, 3639 (1993).

[22] G. Ernst, R. J. Haug, J. Kuhl, K. von Klitzing, and K. Eberl, Phys. Rev. Lett. **77**, 4245 (1996).

[23] V. A. Volkov, D. I. Galchenkov, L. A. Galchenkov, M. Grodnenskii, D. R. Matov, and S. A. Mikhailov, Pisma Zh. Éksp. Teor. Fiz. **44**, 510 (1986) [JETP Lett. **44**, 655 (1986)].

[24] U. Zulicke, R. Bluhm, V. A. Kostelecky, and A. H. MacDonald, Phys. Rev. B **55**, 9800 (1997).